TOPICAL REVIEW — Terahertz physics

Active metasurfaces for manipulatable terahertz technology*

Jing-Yuan Wu(吴静远)[1], Xiao-Feng Xu(徐晓峰)[1], and Lian-Fu Wei(韦联福)[1,2,†]

[1] Photonics Laboratory and Institute of Functional Materials, College of Science, Donghua University, Shanghai 201620, China
[2] Information Quantum Technology Laboratory, School of Information Science and Technology, Southwest Jiaotong University, Chengdu 610031, China

(Received 18 May 2020; revised manuscript received 28 June 2020; accepted manuscript online 15 July 2020)

Metasurface is a kind of two-dimensional metamaterial with specially designed sub-wavelength unit cells. It consists of single-layer or few-layer stacks of planar structures and possesses certain superior abilities to manipulate the propagating electromagnetic waves, including the terahertz (THz) ones. Compared with the usual passive THz metasurfaces whose optical properties are difficult to be controlled after fabrication, the active materials are highly desirable to enable dynamic and tunable control of THz waves. In this review, we briefly summarize the progress of active THz metasurfaces, from their physical mechanisms on carrier concentration modulations, phase transitions, magneto-optical effects, etc., for various possible THz applications mainly with low-dimensional materials, vanadium dioxide films, and superconductors.

Keywords: metamaterial, active metasurface, terahertz wave modulations

PACS: 42.79.Hp, 41.20.Jb, 87.50.U–, 64.70.Nd **DOI:** 10.1088/1674-1056/aba613

1. Introduction

Terahertz (THz) radiation, with the frequencies spanning over 0.1 THz to 10 THz in electromagnetic spectrum, bridges the gap between high-speed electronics and photonics and shows great potential applications in, such as noncontact imaging, fingerprint chemical identification, high-speed wireless communication, and so on.[1–5] To sufficiently take advantage of THz radiation, the capability to manipulate the fundamental properties of the propagating THz waves, including their amplitude, phase, polarization, etc., is an essential issue. Compared with 3D metamaterials whose characteristics are depending on the gradually accumulated phase of waves propagating inside the bulky media, 2D metasurfaces composed of planar artificial subwavelength unit cells demonstrate much better abilities to mold light flows than bulk metamaterials due to lower absorption.[6–9] Specifically, the reduced fabrication difficulty and better integration flexibility make metasurfaces more suitable to explore new effects in THz physics with various designable functional devices.[10–13]

Usual passive THz metasurfaces are made of noble metals with low non-radiative losses (i.e., ohmic losses) by making use of their excellent conducting properties of THz frequency waves.[14,15] Though the metals support sharp resonances, the properties of these passive metasurfaces are fixed after the fabrications, which restrict the modulation bandwidth and functionalities. One way to realize the dynamic and reconfigurable THz metasurface, i.e., the active one, is by changing the geometrical parameters or the arrangements of unit cell structures.[16,17] Micro-electro-mechanical-systems (MEMS) systems[18,19] as well as flexible substrates[20,21] have been employed to effectively alter the radiation features of THz wave by mechanical actuations. Besides, by utilizing active materials sensitive to external stimuli,[22–24] such as temperature, electrical bias, illumination, magnetic effects, etc., the desired dynamic manipulations of THz waves can be realized. A variety of materials including doped semiconductors,[25–28] graphene,[29–32] vanadium dioxide films,[33–37] superconductors,[38,39] etc. have been demonstrated to be promising candidates for the generation of the active THz metasurfaces.

In this review, we plan to provide a brief survey of THz active metasurfaces enabled by various physical mechanisms in terms of carrier concentration modulation, phase transitions, magneto-optical effects, etc. In Section 2, the carrier concentration modulations in 2D materials, through electrical gating as well as optical excitation, are introduced. Section 3 mainly reviews the mechanisms of phase transitions based on vanadium dioxide and superconductor to manipulate the THz waves. The potential THz modulation by using the magneto-optical metasurface is reviewed in Section 4. Finally, we conclude the review with the perspectives on the future directions of the active THz metasurfaces.

2. Carrier concentration modulation

One of the most common and mature approaches to tune the resonant characteristics of metasurfaces is through the control of the free carrier concentration in conductive materials by

*Project supported by the National Natural Science Foundation of China (Grant No. 11974290) and the Fundamental Research Funds for the Central Universities, China (Grant No. 2232020D-44).

†Corresponding author. E-mail: lfwei@dhu.edu.cn

electrical gating or optical excitation. According to the Drude model, the refractive index of the material can be changed by altering its free carrier concentration via electrical and optical controls.[24,40] The first demonstration of electric control of THz wave transmissions was reported in 2006 by combining doped semiconductors with metal metasurface.[25] Silicon and III–V semiconductors (GaAs, InSb, etc.) are the most commonly used semiconductors for manipulating the THz waves via carrier depletion or accumulation.[41–43] The modulation by metal metasurface devices is usually narrowband due to the resonant nature. While the metasurfaces formed completely from doped semiconductors can exhibit wide and dynamic tunability, as their carrier densities and dielectric constants are adjustable by applying the external electrical and optical stimuli.[44] Moreover, the dielectric metasurface can achieve a gradual spatial variation of the carrier density instead of global modulation.[45,46] New active materials (e.g., 2D electron gas in quantum well and epsilon-near-zero material) are also emerging,[22,27,47] which could be employed to further improve the device performance. Generally speaking, compared with 3D bulky semiconductors, 2D layered materials take more advantages to achieve tunable THz metasurface for THz modulations, due to their controllable band structures and quantum confinement effects.

2.1. Basic properties of typical 2D materials

The 2D materials are layered structures with the thicknesses usually ranging from one atomic level to tens of nanometers, wherein the densities of states are relatively low because the carriers are strongly confined along the out-of-plane directions.[48–50] As a consequence, the carrier concentration change in 2D materials by electrical or optical stimuli could be more remarkable. Moreover, 2D materials are passivated on surface without any dangling bonds, which makes them have excellent compatibility free of lattice mismatch issue, specifically when integrating with other materials or structures.[51–54]

It is well-known that graphene is the first isolated 2D material and it has gained much attention in the last years.[55–58] Due to its gapless band structure with linear dispersion near the K point (Fig. 1(a)), charge carriers in graphene behave as massless Dirac fermions.[59] Therefore, graphene with zero gap possesses ultrahigh electrical conductivity and mobility, such as on the order of 10^5 $cm^2 \cdot V^{-1} \cdot s^{-1}$ at room temperature.[60] In addition, graphene interacts with electromagnetic waves in an ultra-broadband spectrum, ranging from UV to THz.[61,62] Another striking feature of graphene is that it supports surface plasmon with low losses and extremely tight confinement.[63–66] The plasmonic resonance wavelengths of the patterned graphene nanostructures are usually at infrared and THz frequency. More importantly, compared with plasmons in metals, graphene plasmons show higher tunability by modifying the Fermi level. These indicate that graphene is a very promising candidate for designing the desired dynamic THz metasurfaces. On the other hand, MoS_2 is one of the best known transition metal dichalcogenides (TMDC).[49,50] It transits from in-direct bandgap of about 1.2 eV to a direct gap at 1.9 eV when it changes from multilayer to monolayer (Fig. 1(b)), which makes it more suitable to implement field-effect transistors with high on–off ratio and photodetectors for detecting the visible and infrared photons.[67,68] Besides, MoS_2 has shown unique physics such as strong nonlinear response, valley Hall effect, and large excitonic effect.[40] The THz devices with MoS_2 materials are expectable, although rare researches have been reported until now. Typically, the ultrafast carrier dynamics in MoS_2 was demonstrated with the time-resolved spectroscopies,[69–71] including optical pump–optical probe spectroscopy, time-resolved photoluminescence and THz spectroscopy, etc. The photo-response time of monolayer MoS_2 is reported as fast as 350 fs,[70] which indicates that MoS_2 may be utilized to generate the high-speed THz devices.

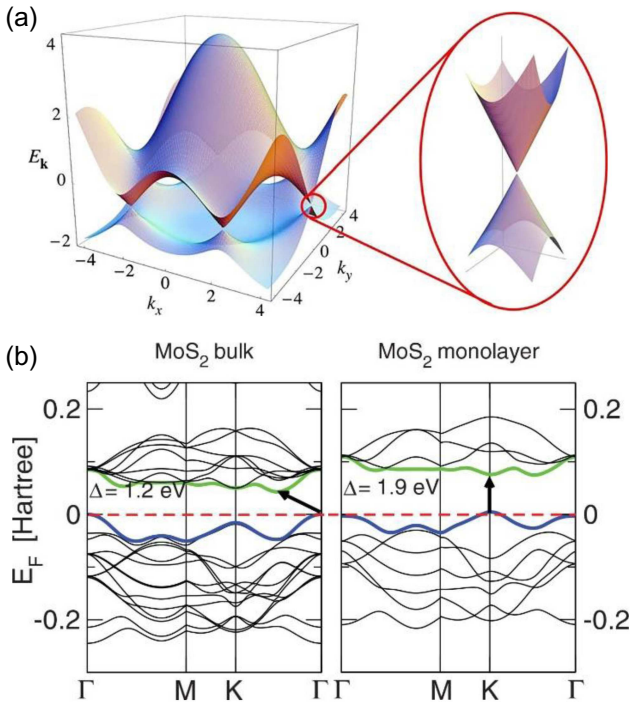

Fig. 1. (a) The electronic dispersion of graphene. (b) Calculated band structures of bulk MoS_2 and monolayer MoS_2. The arrows indicate the indirect and direct bandgaps, respectively. (a) Reproduced with permission from Ref. [59]. Copyright 2009, APS. (b) Reproduced with permission from Ref. [50]. Copyright 2011, APS.

2.2. Active THz metasurface based on 2D material

Since the early 2010s, graphene has been investigated for the active control of the THz radiation. Generally, THz metasurfaces based on graphene can be constructed in two ways.

The first one is integrating graphene with either metallic or dielectric metasurfaces and thus the resonant characteristics of the metasurfaces could be controlled by electrically tuning the carrier density of graphene.[32,72–74] It plays a similar role in the metasurfaces generated by the traditional doped semiconductors. Specifically, Lee *et al.* proposed a gate-controlled THz graphene metasurface,[72] in which graphene was integrated with a hexagonal gold antenna array and the dimensions and spacing of the metallic arrays were designed to realize extraordinary optical transmission. The highest amplitude modulation depth of 47% and phase change of 32.2° were observed. Also, a gate-controlled graphene THz metasurface was demonstrated to realize an active phase control (Fig. 2(a)).[73] Graphene was utilized to tune the damping of the resonator and the value of phase variation reached 2π across its resonant frequency (Figs. 2(b) and 2(c)). In addition to the amplitude and phase modulation, several studies focused on the active tuning of polarization and resonant frequency.[75–77] For example, Kindness *et al.* employed metal-coupled resonator arrays that exhibit an electromagnetically induced transparency to integrate with graphene (Fig. 2(d)).[76] By applying an electrical bias to graphene, one of the resonators can be damped and consequently, the resonance frequency of the metasurface can be tuned in a wide range of about 100 GHz as shown in Fig. 2(e).

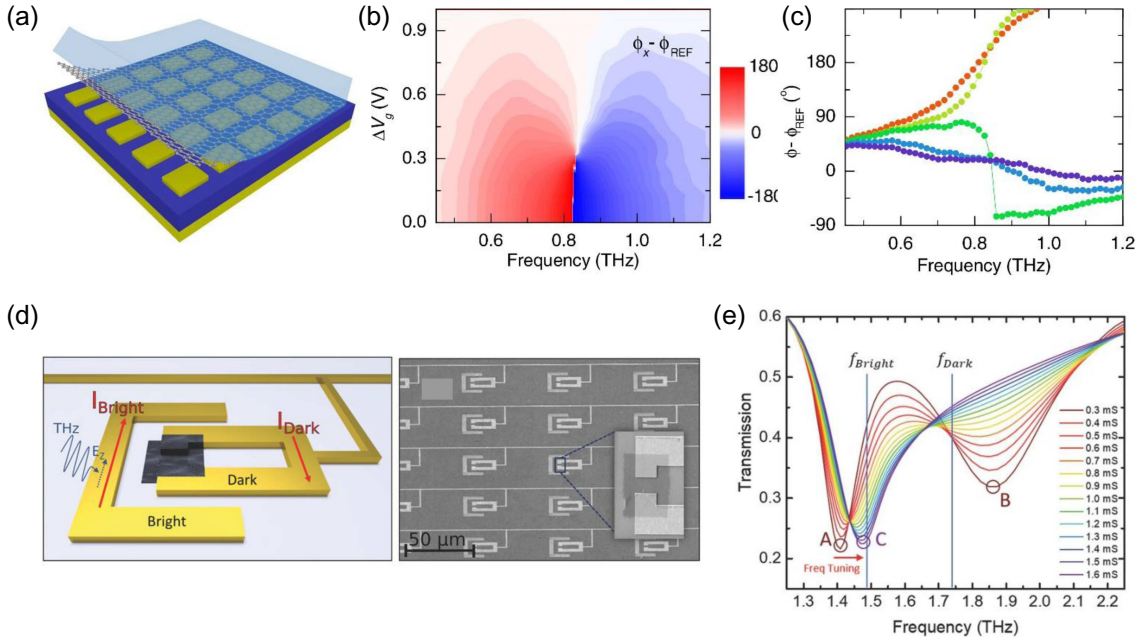

Fig. 2. (a) Schematics of the metasurface with the graphene transferred onto the array of Al mesas. (b) Phase modulation performance measured at different frequencies and gate biases. (c) The phase difference between waves at different polarizations. (d) Representation of coupled resonator structure. (e) The simulated transmission through the resonator as a function of frequency at different values of graphene conductivity. (a)–(c) Reproduced with permission from Ref. [73]. Copyright 2015, APS. (d), (e) Reproduced with permission from Ref. [76]. Copyright 2018, Wiley-VCH.

Another way to realize the metasurface is by patterning graphene itself, which supports surface plasmon polariton in THz frequency.[66] In fact, a variety of fabrication methods have been developed to realize the patterned graphene,[78] mainly by the top-down technique[79–82] (electron beam lithography, nono-imprint lithography, inkjet printing, etc.) and the bottom-up one[83–85] (self-assembly, plasma enhanced chemical vapor deposition, etc.). For example, Yatooshi *et al.* designed a metasurface by putting graphene ribbon arrays onto a silver mirror and realized the control of the reflected THz wavefront (Figs. 3(a) and 3(b)).[86] By tuning the localized plasmon resonances of patterned graphene via changing the Fermi level, the THz modulation was implemented due to the abrupt phase shifts of the metasurfaces. The relevant numerical simulations indicated that the THz wave beam can be deflected up to 53° with a reflection efficiency of 60%, and the switching time is shorter than 0.6 ps. In addition to the ribbons, other geometries of plasmonic structures[87–89] could also be utilized, including the disks, holes, dots, etc. It is noted that, apart from direct patterning presented above, the graphene plasmonic metasurface can also be generated by electrically doping the whole sheet. Typically, for example, Huidobro *et al.* realized the anisotropic and isotropic plasmonic metasurfaces by periodically modulating the metasurfaces along one and two directions, respectively.[90] To increase the light–matter interaction for enhancing the modulation depth, graphene metasurface is expected to integrate with resonant plasmonic structures or microcavities.[91–93] In a typical example, 60% of transmission modulation with the modulated speed of 40 MHz, as shown in Figs. 3(c) and 3(d). was demonstrated by integrating graphene resonators with metallic antennas arrays.[94]

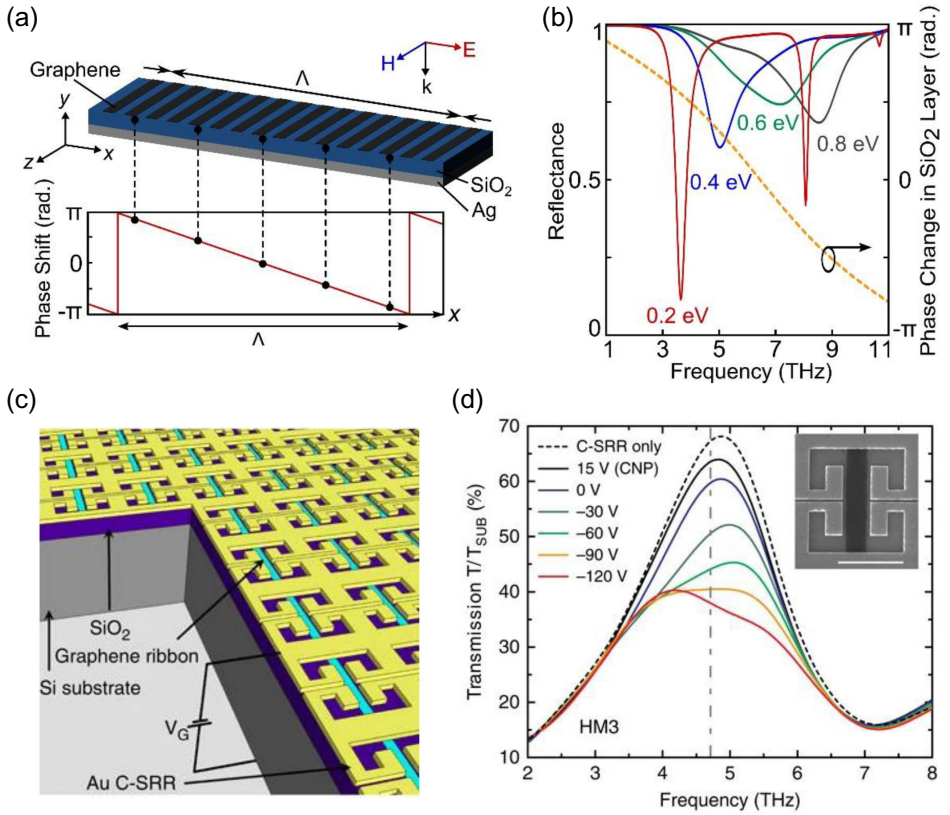

Fig. 3. (a) Illustration of a tunable metasurface consisting of graphene ribbons on a Ag mirror with a SiO_2 gap layer. (b) Simulation result of reflectance spectra at different Fermi levels for the TM polarization. (c) 3D schematic representation of the complementary split-ring resonators-graphene hybrid metasurface on a SiO_2/Si substrate. (d) The transmission modulation of the device operating at 4.5 THz. (a), (b) Reproduced with permission from Ref. [86]. Copyright 2015, AIP. (c), (d) Reproduced with permission from Ref. [94]. Copyright 2015, Springer Nature.

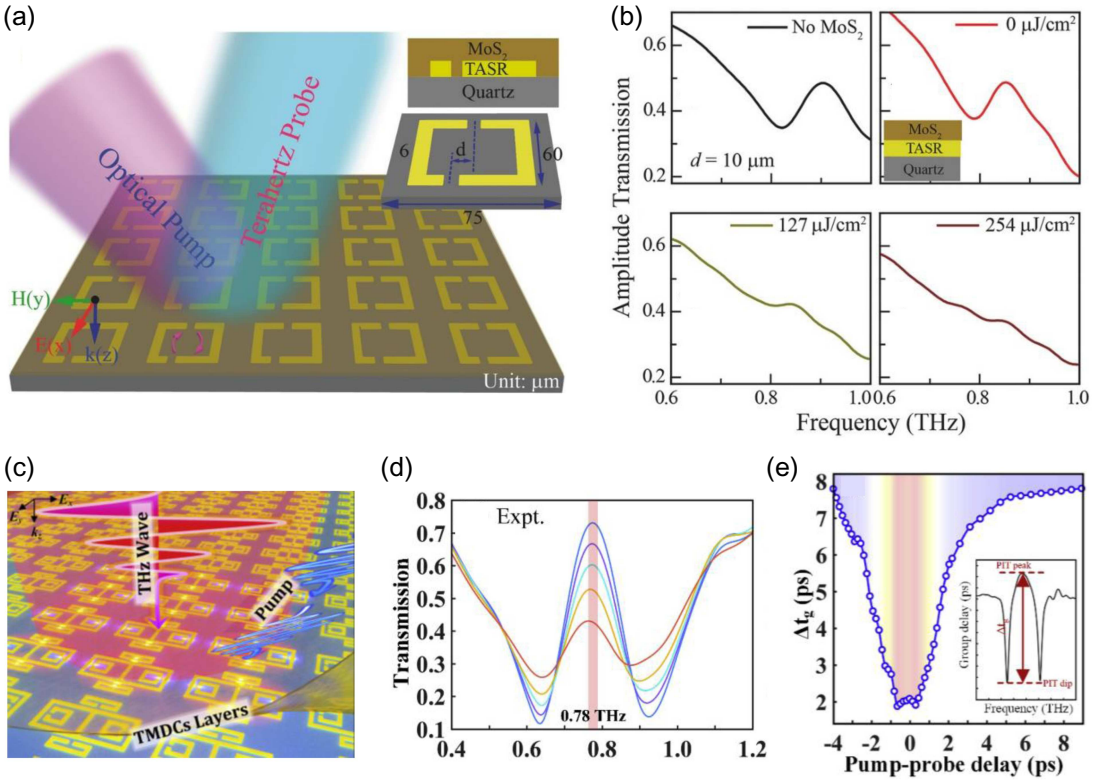

Fig. 4. (a) Schematic of multilayer MoS_2 dropped casted on asymmetric resonator under the illumination of the optical pump and THz probe pulses. The inset shows the cross-section of the unit cell. (b) Measured terahertz transmission spectra without MoS_2 and with MoS_2 at different optical pump fluences. (c) Schematic of WSe_2 covered metasurface. (d) Power dependence of the THz transmission at different pump fluences. (e) Transient evolution of the ultrafast THz switching metasurface. (a), (b) Reproduced with permission from Ref. [96]. Copyright 2017, Wiley-VCH. (c)–(e) Reproduced with permission from Ref. [97]. Copyright 2020, Elsevier.

The study on the other 2D materials based hybrid metasurfaces in the THz range is probably desirable, although it is still in the initial stage. Note that, owing to the bandgap resonance,[95] the optical absorption of MoS_2 (10%) is larger than that of graphene, the all-optical modulator generated by MoS_2 and other TMDC might possess the lower insertion loss and the larger modulation depth, compared with that made by graphene in principle. By utilizing MoS_2-coated metasurface,[96] Srivastava *et al.* have demonstrated ultrasensitive switching and Fano resonance modulation of THz wave (Fig. 4(a)). The modulation depth up to 100% was observed with the pump power of 200 mW (Fig. 4(b)). The switch was found at the time scale of 100 ps in the optical pump-THz probe measurement. In their experiment, the multilayer MoS_2 is prepared by drop-casting method and its photoconductivity is significantly enhanced compared with the monolayer counterpart. Very recently, Hu *et al.* transferred a WSe_2 multilayer prepared by chemical vapor deposition method on a plasmon-induced transparency metasurface, and the transmission amplitude modulation was 43% with the switching of slow light up to 6 ps at 0.78 THz (Figs. 4(c)–4(e)).[97]

3. Phase transition material induced active tuning

3.1. Vanadium dioxide

3.1.1. Investigation of phase transition in VO_2

Vanadium dioxide (VO_2) is a kind of strongly correlated materials.[98–100] At a transition temperature of about 340 K, the insulator-to-metal transition (IMT) takes place, i.e, its lattice structure is transited from the monoclinic (insulating phase) to the rutile (metallic phase). By the characterization of high resolution transmission electron microscopy (HRTEM) (Fig. 5(a)), He *et al.* showed the dynamic domain wall motion of VO_2 IMT directly and provided the visualized information, at atomic level, about the structural features of VO_2 during the phase transition process.[101] The result reflected that the domain wall positions are exactly located in (202) and (040) planes of rutile structure after phase change at the temperature of 50 °C. In addition to the thermal heating, a variety of triggering methods,[102–105] including electric field, optical excitation, magnetic field, etc., have also been demonstrated to realize the IMT with VO_2. Figures 5(b) and 5(c) show that the external electric field can directly induce the phase transition in a sandwich VO_2 layer.[103]

Recent developments in the field of intense THz wave generation have promoted the research of charge carrier dynamics in VO_2.[106] By combining it with plasmonic structures which provide field enhancement, the IMT of VO_2 driven by the THz field was first observed in 2012 by Liu *et al.*[107] It is also helpful to have a better understanding of the IMT mechanisms involving structural and electronic transitions (Fig. 6(a)) by utilizing the THz nano antennas. It was argued that the non-thermal field-driven IMT of VO_2 makes little contribution to the conductivity changes.[108] As shown in Fig. 6(b), Gray *et al.* also employed THz excitation to achieve the IMT,[109] probed by the near-IR spectroscopy combing with x-ray scattering measurement. The experimental result further demonstrated that the electric-field-induced electronic and structural phase transitions occur on different timescales.

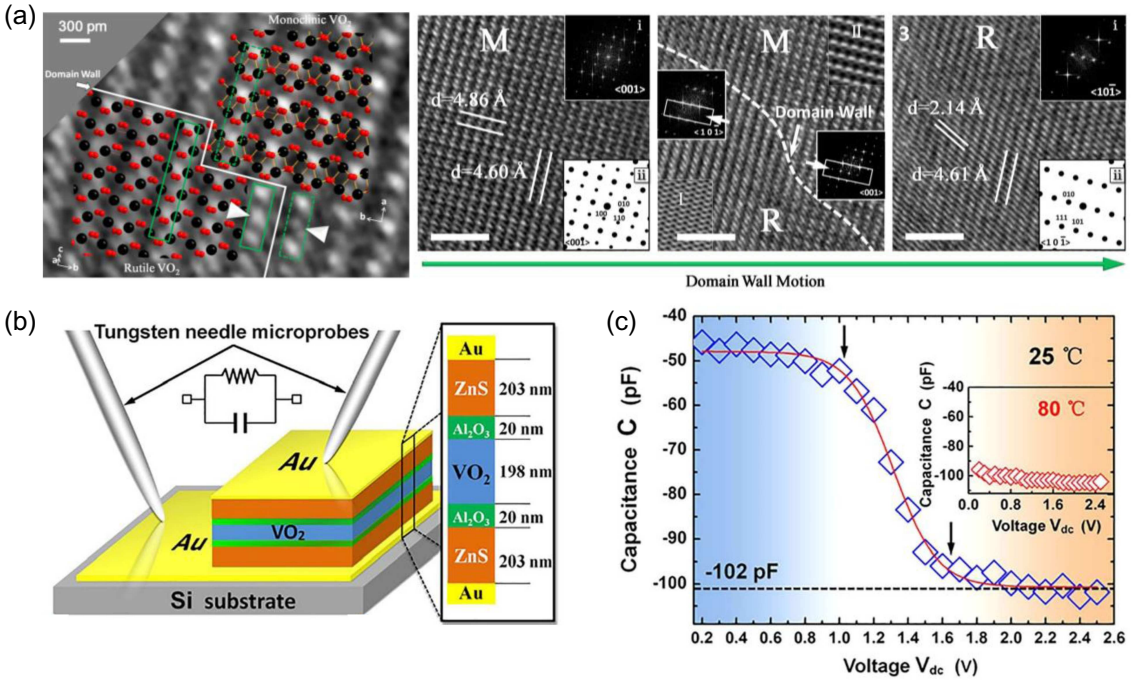

Fig. 5. (a) HRTEM image of monoclinic/rutile domain walls in VO_2 and *in situ* domain wall motion observation of monoclinic VO_2 at 25 °C, 50 °C, and 70 °C. (b) Quantum well structure with a sandwich VO_2 layer. (c) Capacitance changes with the dc voltage at 25 °C. Inset shows the capacitance,-voltage curve at 80 °C. (a) Reproduced with permission from Ref. [101], copyright 2014, Springer Nature. (b), (c) Reproduced with permission from Ref. [103], copyright 2015, AIP.

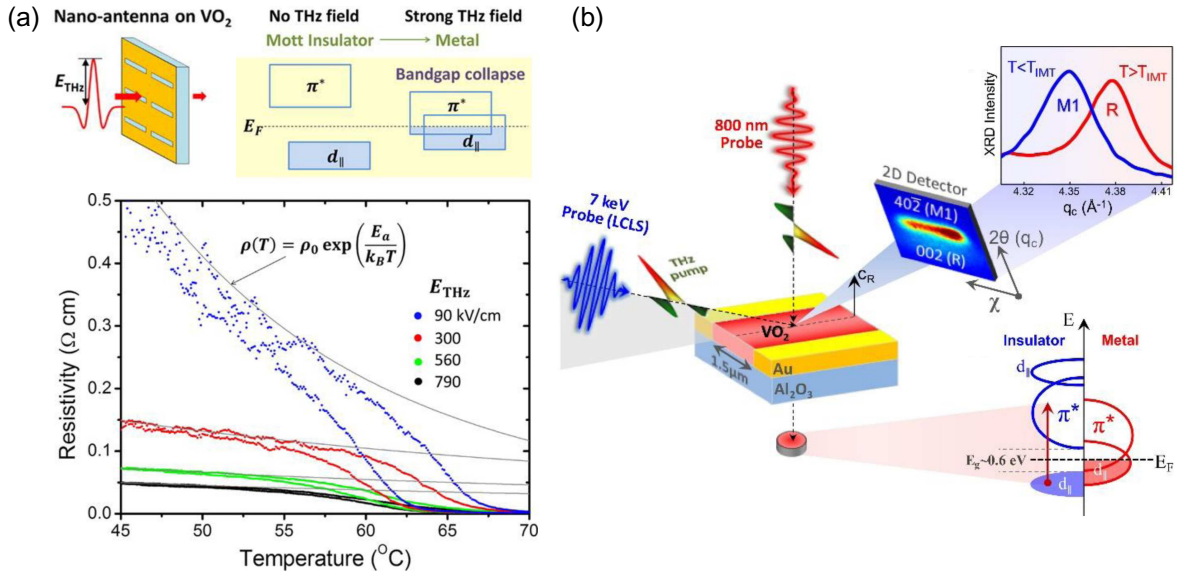

Fig. 6. (a) Schematic energy diagram for THz-driven IMT in VO_2 and resistivity hysteresis curves. (b) Illustration of the THz-pump/x-ray probe experiment and the relevant observable processes. (a) Reproduced with permission from Ref. [108], copyright 2015, ACS. (b) Reproduced with permission from Ref. [109], copyright 2018, APS.

3.1.2. Active THz metasurface based on VO_2

Undoubtedly, VO_2 has become one of the attractive candidates to construct the desired tunable metasurfaces, although the precise microscopic origin of IMT in VO_2 is still under debate. The reasons are as follows. First, VO_2 presents a giant change of conductivity (three to four orders of magnitude) at THz frequency[110] after the IMT-triggering stimuli. Besides, compared with other phase-change materials,[111] it exhibits relatively low transition temperature in terms of thermal stimuli. Second, according to the ultrafast carrier dynamics experimental observations, VO_2 is promising to realize ultrafast THz all-optical modulation with the response time in the order of picoseconds.[109] Thirdly, a lot of mature methods,[112–116] including magnetron sputtering, pulsed laser deposition, etc., have been developed to prepare large-area VO_2 films with high qualities. This has promoted the experimental generations of the VO_2 metasurfaces with different structures. Thermal heating has been widely used to generate VO_2-based active THz metasurfaces for various realistic applications.[37,117–120] In 2010, an active THz nano antenna operated by heating the VO_2 film was proposed (Fig. 7(a)).[33] It was shown that the spectral range of the THz transmission reads from 0.2 THz to 2 THz, if the VO_2 is in the insulating phase. Inversely, if VO_2 was converted into the metallic phase by heating, the intensity of the THz transmission is dramatically reduced. Basically, VO_2 could also be patterned to form metasurface without any metal nanostructures.[121] The THz metasurface composed of VO_2 cut-wires was fabricated and the VO_2 resonator, after phase transition, could act as metallic antennas to increase the absorption at the resonance frequency.[122] Besides the thermally controlled manner, the electrical and photoinduced active THz metasurfaces with a combination of VO_2 and metal metasurface have also been investigated recently.[123–126] For example, Cai *et al.* demonstrated a VO_2 based metadevice to realize the THz wave controls via electrical driven manner and ultrafast optical pumping, respectively (Fig. 7(b)).[124] The VO_2 patterns were incorporated within the gap between the asymmetric split-ring resonators. As a result, a modulation depth of 54% and a switching time of 2.2 s were demonstrated under the electrically triggering with a reduced operation temperature. A faster switching within 30 ps was achieved by the all-optical modulation using the femtosecond pulse excitations. Also, the photoinduced phase change of VO_2 can be utilized to generate a phase shift of THz wave, for example, integrating VO_2 nanostructures with the ring-dumbbell metal antenna was proposed.[123] By varying the power of the applied laser, the phase shift exceeding 130° near 0.6 THz was observed (Fig. 7(c)). Hopefully, the VO_2-based active metasurfaces are useful to generate the robust multifunctional THz optoelectronic devices,[13,127–130] including the photonic memory and linear polarizers, for the THz sensing and imaging applications.

3.2. Superconductor

The excellent phase-transition performance of a superconductor originates from its low ohmic loss below the critical temperature (T_c).[131,132] The superconductors are highly utilized in the field of metamaterials/metasurfaces, due to their several unique properties including the zero electrical resistance, perfect diamagnetism, excellent tunable capability, inherent nonlinearity, and quantum effects such as Josephson tunneling and flux quantization.[133–136] It is noted that different resonance line shapes (Lorentzian and Fano resonances) of the THz metasurface superconducting resonators were investigated by Srivastava *et al.*[137] The observed Lorentzian and Fano resonance line shapes correspond to the dominant

radiative and ohmic losses, respectively. The resonator was made by the yttrium barium copper oxide (YBCO), one of the best known high-temperature superconductors. For the Lorentzian type, YBCO and metal show similar resonance responses, as high radiative losses suppress the conductivity change. However, for the asymmetric Fano resonance, the conductivity strongly affects the quality (Q) factor of the resonator (Fig. 8). This implies that high-T_c superconductors provide a better basis to obtain ultrahigh-Q resonances in THz Fano resonant metasurfaces compared with metal. Furthermore, Zhang *et al.* also demonstrated an unloaded Q factor 24 times larger than that of gold metasurface in the NbN superconducting resonator.[138] This means that the active THz metasurfaces generated by the low-temperature superconductors are also expectable for THz modulations.

The complex conductivity of superconductor could also be tunable by controlling the temperature variation, electrical bias, optical excitation, or magnetic field.[134,139–141] The range of the resonant frequency is significantly wide. Chen *et al.* demonstrated such a tunability with the YBCO metasurfaces by reducing the temperature (Fig. 9(a)).[142] In a parallel line, Nb and NbN were also reported to realize THz metasurface with temperature-dependent resonance behavior. Besides,

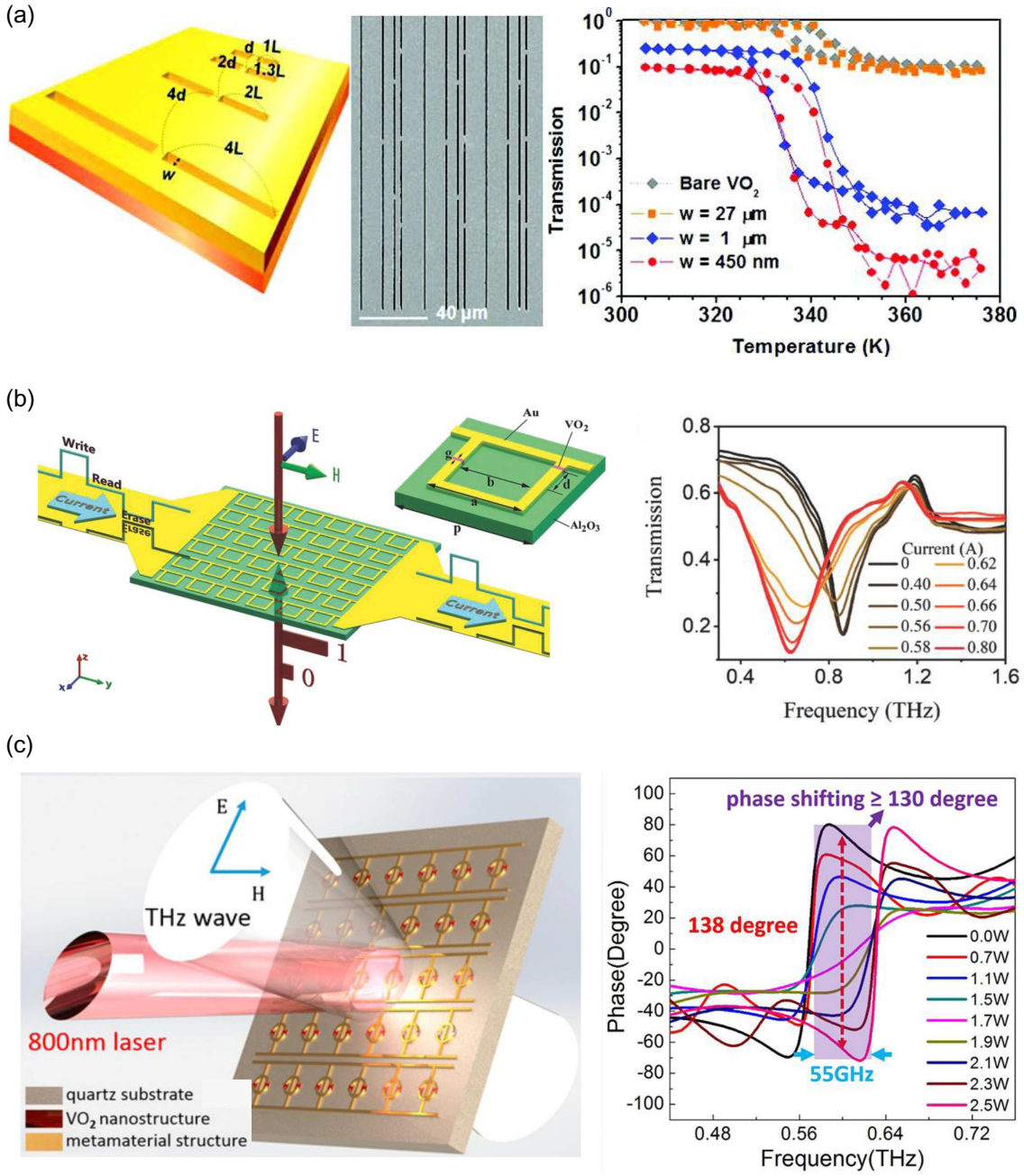

Fig. 7. (a) Illustrations of metasurface with metal resonator patterns on a VO_2 film and the transmission spectra at different temperatures. (b) Diagram of the VO_2 based hybrid metasurface and the transmission spectra at different values of electric current. (c) The sketch of the metasurface and phase spectra with the increasing light power. (a) Reproduced with permission from Ref. [33], copyright 2010, ACS. (b) Reproduced with permission from Ref. [124], copyright 2018, Wiley-VCH. (c) Reproduced with permission from Ref. [123], copyright 2018, ACS.

superconducting material can be employed to achieve electromagnetically induced transparency, see, e.g., Fig. 9(b) for the planar THz metasurface fabricated with NbN films.[143] The temperature-dependent THz transmission spectra (Fig. 9(c)) present two resonance dips below the critical temperature of 16 K. The resonance becomes stronger with the decrease of the temperature, exhibiting a higher Q factor. All-optical ultrafast tuning of inductive-capacitive resonant metasurface based on YBCO with switching speed of few picoseconds was also demonstrated by Srivastava *et al.* (Fig. 9(d)).[144] The reported ultrafast devices demonstrating good performance are useful for the future THz high-speed wireless communication.[145]

In terms of the nonlinear response, the transmission spectra of metasurface based on superconductors in THz regime show a power-dependent characteristic, as the strong electric field changes the number of Cooper pairs. A typical example is shown in Figs. 10(a)–10(c), NbN film based metasurface exhibited a nonlinear THz transmission below the critical temperature under the excitation of intense THz field.[133] When the temperature increased to T_c, the nonlinearity turned to be weak due to the influence of thermal agitation. A nonlinear THz response also happens in the YBCO based metasurface (Figs. 10(d) and 10(e)).[146] In addition, superconducting metasurface with quantum effects has also gradually gained attention.[147,148]

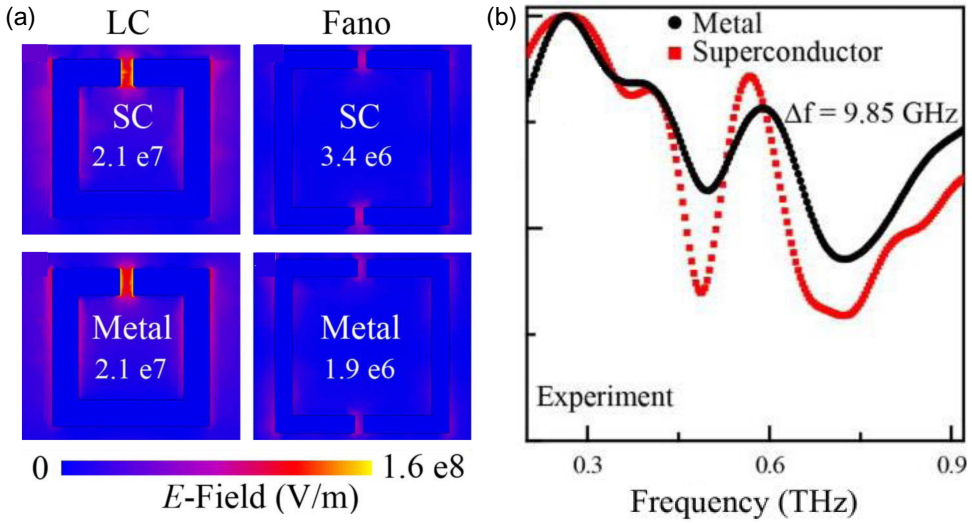

Fig. 8. (a) Electric field distribution in Lorentzian and Fano resonators for YBCO and aluminum, respectively, the optical image of the fabricated Fano resonator samples. (b) Measured amplitude transmission spectra. (a), (b) Reproduced with permission from Ref. [137], copyright 2017, AIP.

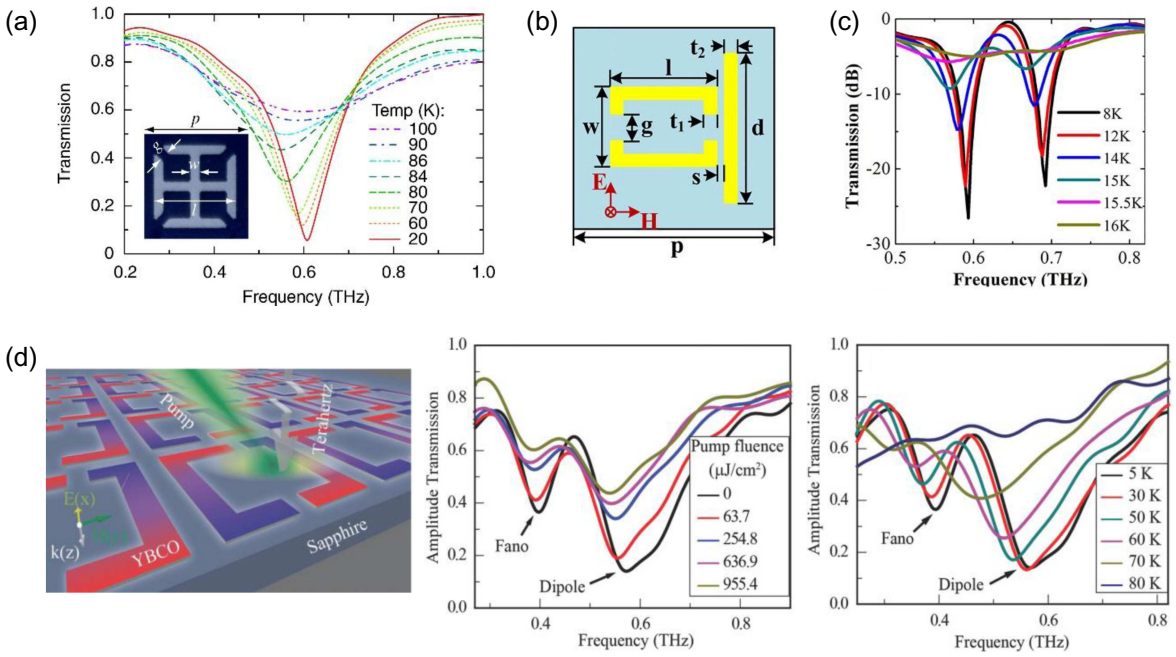

Fig. 9. (a) Measured transmission amplitude spectrum of the metasurface at different temperatures. (b) Planar geometry of NbN based metasurface. (c) THz transmission spectra at different temperatures. (d) Ultra-fast all-optical switch based on YBCO hybrid metasurface. (a) Reproduced with permission from Ref. [142], copyright 2010, APS. (b), (c) Reproduced with permission from Ref. [143], copyright 2011, AIP. (d) Reproduced with permission from Ref. [144], copyright 2018, Wiley-VCH.

For example, the Meissner effect at terahertz frequencies has a broad range of implications in realizing quantum metasurfaces without Josephson junction. More interestingly, quantum metasurface could manipulate the quantum properties of the propagating waves, which is useful to generate and detect the photonic entanglement.[149] Therefore, the quantum metasurfaces possess the great potential in quantum information processings, quantum interferences, and also the perfect photon detectors.[150] Additionally, it is expected that the quantum metasurfaces might be applied to implement ultrafast quantum switching and thereby realize low-loss and ultrasensitive switchable quantum devices operating at THz frequencies.

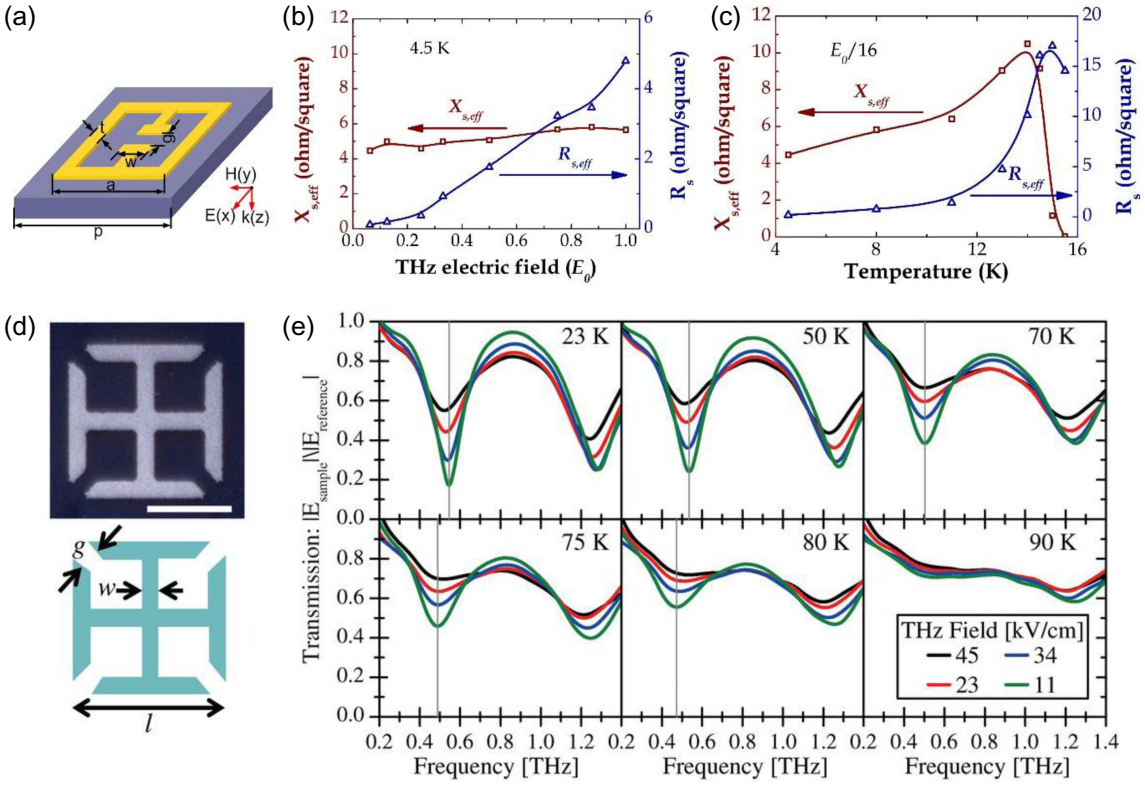

Fig. 10. (a) Schematic of a superconducting NbN metasurface. (b) Effective surface reactance and resistance as a function of THz electrical field and (c) as a function of temperature. (d) The THz metasurface in which the light area is YBCO and the dark area is $LaAlO_3$ substrate. (e) THz field strength-dependent transmission spectra at different temperatures. (a)–(c) Reproduced with permission from Ref. [133], copyright 2013, AIP. (d), (e) Reproduced with permission from Ref. [146], copyright 2013, IOP.

4. Magneto-optical effect

4.1. Properties of magneto-optical materials in THz regime

Generally, magnetic field is difficult to realize active metasurface compared with other external stimuli, as the effect of magnetic field on the optical materials is relatively weak. However, combining metasurface with magneto-optical (MO) materials could not only significantly enhance the MO effect by plasmonic resonance, but also lead to some novel physical phenomena, such as plasmonic resonance splitting, nonreciprocal propagation, etc.[151] In visible regime, MO approach has been widely implemented to realize chiro-optical metasurfaces.[152,153] However, suitable MO materials with significant MO effect and low loss in THz regime are relatively rare. Semiconductors of high electron mobility with the cyclotron frequency locating in the THz frequency range, for example, InSb, have been served as the MO materials.[151] While MO Faraday and Kerr rotations have been experimentally reported in graphene ranging from far-infrared to microwave frequency.[154] Therefore, graphene is of great potential for THz MO modulation.

4.2. THz MO modulation devices

MO material with outstanding non-reciprocal transmission provides the possibility to realize various functional devices that are not feasible based on other modulation principles. Specifically, THz MO modulators may apply to optical isolators, polarization controllers, magnetic-field sensors, etc. For example, as a typical nonreciprocal one-way transmission device with the broken time-reversal symmetry, the isolator is of great importance to suppress the noise induced by the reflection and scattering of THz waves. A periodically patterned InSb layer coated on the silica substrate has been demonstrated to generate a THz MO metasurface isolator (Fig. 11(a)).[155] Due to the asymmetry structure along the incident polarization direction of the THz wave, the magnetoplasmonic mode splits with an enhanced nonreciprocal resonance (Fig. 11(b)).

The MO metasurface with similar structures had been utilized to act as a magnetic field sensor by making use of the relationship between the resonant frequency and the applied external magnetic field.[156] Usually, due to the high absorption, the MO device based on InSb and the other bulk materials cannot operate at the frequencies above 1.5 THz. However, with a hybrid metasurface integrated graphene with an array of split-ring resonators (Fig. 11(c)), Ottomaniello *et al.* showed that large non-reciprocal polarization rotation can be achieved over a broad range of frequencies (larger than 1 THz).[157]

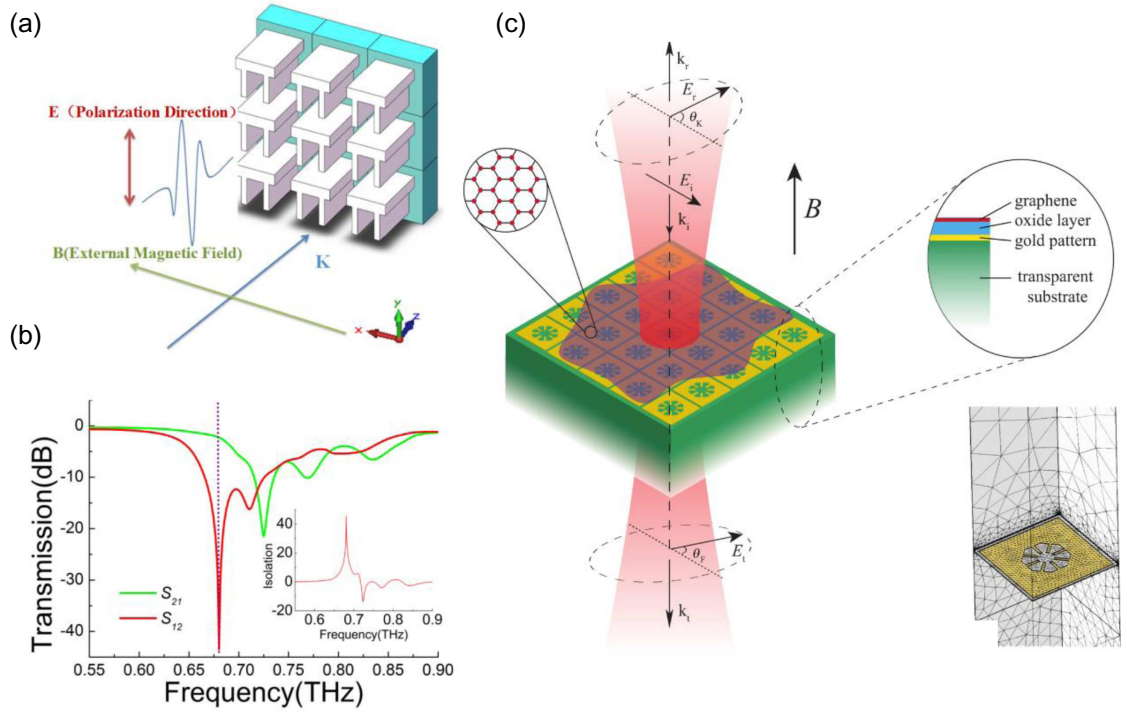

Fig. 11. (a) Schematic structure of isolator based on the MO metasurface. (b) The transmission spectrum of the forward waves and backward waves at $T = 195$ K and $B = 0.3$ T, respectively. The inset shows the isolation spectra of the isolator. (c) The sketch of the hybrid metasurface composed of a monolayer graphene and gold array separated by SiO_2 layer. (a), (b) Reproduced with permission from Ref. [155], copyright 2015, OSA. (c) Reproduced with permission from Ref. [157], copyright 2018, OSA.

5. Conclusion and perspectives

In this review, we have briefly summarized the realization of dynamic THz wave control based on active materials. The efficient manipulation of THz waves in terms of their spectral and spatial characteristics is essential for THz technology. The evolution from the passive metasurface to the active ones has provided significantly expanded capabilities and functionalities. We have witnessed the repaid development of the dynamic THz wave manipulation so far, involving the emergence of different kinds of active materials (e.g. 2D materials, various phase-change materials) as well as novel structures and tuning mechanisms. This is useful for further improving the modulation performance of the THz wave and pursuing the application of the active THz metasurfaces in the single-pixel THz imaging, 6G wireless communication, etc.[158,159]

In the following, we would like to suggest several directions moving forward in this field. First, for the real application of THz metasurface, it is necessary to independently address and activate each sub-wavelength unit cell in a large number, i.e., pixelated manipulation of THz waves.[22] However, until now, most of the reported active metasurfaces are homogeneous which are tuned uniformly or the number of pixels is too small to compete, due to the lack of suitable voltage-driven miniaturized element in THz regime. The further efforts could be paid to designing inhomogeneous metasurfaces based on new physics and improving the fabrication technology in terms of high integration and low power consumption. Second, apart from the spectral and spatial modulations, the extra temporal control at an ultrafast speed has gained much attention recently, as it relates to certain new physical effects. The interaction between ultra-short THz pulse and active materials (e.g., graphene and the other 2D materials) could be explored by taking the non-linear optical effect into consideration.[160,161] This may bring forth a new understanding of light–matter interaction and broaden the high-speed THz applications. Thirdly, the majority of the THz metasurface researches until now are mainly based on the classical electrodynamics. In the future, active quantum metasurfaces (e.g., superconductor hybrid quantum metasurface, TMDC based quantum metasurface) may take an important role in modulating the THz waves at quantum level by developing the relevant THz photonic devices.[148,162,163]

References

[1] Tonouchi M 2007 *Nat. Photon.* **1** 97
[2] Rahm M, Li J S and Padilla W J 2013 *J. Infrared, Millimeter, Terahertz Waves* **34** 1
[3] Koenig S, Lopez-Diaz D, Antes J, Boes F, Henneberger R, Leuther A, Tessmann A, Schmogrow R, Hillerkuss D, Palmer R, Zwick T, Koos C, Freude W, Ambacher O, Leuthold J and Kallfass I 2013 *Nat. Photon.* **7** 977
[4] Wade C G, Šibali N, De Melo N R, Kondo J M, Adams C S and Weatherill K J 2017 *Nat. Photon.* **11** 40
[5] Zhou T, Zhang R, Yao C, Fu Z L, Shao D X and Cao J C 2017 *Chin. Phys. Lett.* **34** 084206
[6] Li A, Singh S and Sievenpiper D 2018 *Nanophotonics* **7** 989
[7] He Q, Sun S and Zhou L 2019 *Research* **2019** 1849272
[8] Glybovski S B, Tretyakov S A, Belov P A, Kivshar Y S and Simovski C R 2016 *Phys. Rep.* **634** 1
[9] Su D, Zhang X Y, Ma Y L, Shan F, Wu J Y, Fu X C, Zhang L J, Yuan K Q and Zhang T 2018 *IEEE Photon. J.* **10** 4600109
[10] Zhang X, Tian Z, Yue W, Gu J, Zhang S, Han J and Zhang W 2013 *Adv. Mater.* **25** 4567
[11] Yu N and Capasso F 2014 *Nat. Mater.* **13** 139
[12] Sun L, Zhou Z, Zhong J, Shi Z, Mao Y, Li H, Cao J and Tao T H 2020 *Small* **16** 2000294
[13] Li J, Yang Y, Li J, Zhang Y, Zhang Z, Zhao H, Li F, Tang T, Dai H and Yao J 2020 *Adv. Theory Simulations* **3** 1900183
[14] Seo M A, Park H R, Koo S M, Park D J, Kang J H, Suwal O K, Choi S S, Planken P C M, Park G S, Park N K, Park Q H and Kim D S 2009 *Nat. Photon.* **3** 152
[15] Luk'Yanchuk B, Zheludev N I, Maier S A, Halas N J, Nordlander P, Giessen H and Chong C T 2010 *Nat. Mater.* **9** 707
[16] Tao H, Strikwerda A C, Fan K, Padilla W J, Zhang X and Averitt R D 2009 *Phys. Rev. Lett.* **103** 147401
[17] Ou J Y, Plum E, Jiang L and Zheludev N I 2011 *Nano Lett.* **11** 2142
[18] Fu Y H, Liu A Q, Zhu W M, Zhang X M, Tsai D P, Zhang J B, Mei T, Tao J F, Guo H C, Zhang X H, Teng J H, Zheludev N I, Lo G Q and Kwong D L 2011 *Adv. Funct. Mater.* **21** 3589
[19] Cong L, Pitchappa P, Lee C and Singh R 2017 *Adv. Mater.* **29** 1700733
[20] Khodasevych I E, Shah C M, Sriram S, Bhaskaran M, Withayachumnankul W, Ung B S Y, Lin H, Rowe W S T, Abbott D and Mitchell A 2012 *Appl. Phys. Lett.* **100** 061101
[21] Ma F, Lin Y S, Zhang X and Lee C 2014 *Light: Sci. Appl.* **3** e171
[22] Shaltout A M, Shalaev V M and Brongersma M L 2019 *Science* **364** eaat3100
[23] Cui T, Bai B and Sun H B 2019 *Adv. Funct. Mater.* **29** 1806692
[24] Wang L, Zhang Y, Guo X, Chen T, Liang H, Hao X, Hou X, Kou W, Zhao Y, Zhou T, Liang S and Yang Z 2019 *Nanomaterials* **9** 965
[25] Chen H T, Padilla W J, Zide J M O, Gossard A C, Taylor A J and Averitt R D 2006 *Nature* **444** 597
[26] Chen H T, Padilla W J, Cich M J, Azad A K, Averitt R D and Taylor A J 2009 *Nat. Photon.* **3** 148
[27] Zhang Y, Qiao S, Liang S, Wu Z, Yang Z, Feng Z, Sun H, Zhou Y, Sun L, Chen Z, Zou X, Zhang B, Hu J, Li S, Chen Q, Li L, Xu G, Zhao Y and Liu S 2015 *Nano Lett.* **15** 3501
[28] Shcherbakov M R, Liu S, Zubyuk V V., Vaskin A, Vabishchevich P P, Keeler G, Pertsch T, Dolgova T V., Staude I, Brener I and Fedyanin A A 2017 *Nat. Commun.* **8** 17
[29] Du L L, Li Q, Li S X, Hu F R, Xiong X M, Li Y F, Zhang W T and Han J G 2016 *Chin. Phys. B* **25** 027301
[30] Gopalan P and Sensale-Rodriguez B 2020 *Adv. Opt. Mater.* **8** 1900550
[31] Zhao Y T, Wu B, Huang B J and Cheng Q 2017 *Opt. Express* **25** 7161
[32] Shi S F, Zeng B, Han H L, Hong X, Tsai H Z, Jung H S and Zettl A 2015 *Nano Lett.* **15** 372
[33] Seo M, Kyoung J, Park H, Koo S, Kim H S, Bernien H, Kim B J, Choe J H, Ahn Y H, Kim H T, Park N, Park Q H, Ahn K and Kim D S 2010 *Nano Lett.* **10** 2064
[34] Zhao S, Hu F, Xu X, Jiang M, Zhang W, Yin S and Jiang W 2019 *Chin. Phys. B* **28** 054203
[35] Zhu H F, Du L H, Li J, Shi Q W, Peng B, Li Z R, Huang W X and Zhu L G 2018 *Appl. Phys. Lett.* **112** 081103
[36] Song Z, Wang K, Li J and Liu Q H 2018 *Opt. Express* **26** 7148
[37] Parrott E P J, Han C, Yan F, Humbert G, Bessaudou A, Crunteanu A and Pickwell-MacPherson E 2016 *Nanotechnology* **27** 205206
[38] Scalari G, Maissen C, Cibella S, Leoni R and Faist J 2014 *Appl. Phys. Lett.* **105** 261104
[39] Keller J, Scalari G, Appugliese F, Mavrona E, Rajabali S, Süess M J, Beck M and Faist J 2018 *ACS Photon.* **5** 3977
[40] Yu S, Wu X, Wang Y, Guo X and Tong L 2017 *Adv. Mater.* **29** 1606128
[41] Alvear-Cabezón E, Smaali R, Centeno E, Gonzalez-Posada F and Taliercio T 2018 *Phys. Rev. B* **98** 035305
[42] Fan Z F, Tan Z Y, Wan W J, Xin X, Lin X, Jin Z M, Cao J C and Ma G H 2017 *Acta Phys. Sin.* **66** 087801 (in Chinese)
[43] Gu J, Singh R, Liu X, Zhang X, Ma Y, Zhang S, Maier S A, Tian Z, Azad A K, Chen H T, Taylor A J, Han J and Zhang W 2012 *Nat. Commun.* **3** 1151
[44] Cai H, Huang Q, Hu X, Liu Y, Fu Z, Zhao Y, He H and Lu Y 2018 *Adv. Opt. Mater.* **6** 1800143
[45] Kamaraju N, Rubano A, Jian L, Saha S, Venkatesan T, Nötzold J, Kramer Campen R, Wolf M and Kampfrath T 2014 *Light: Sci. Appl.* **3** e155
[46] Yang Y, Kamaraju N, Campione S, Liu S, Reno J L, Sinclair M B, Prasankumar R P and Brener I 2017 *ACS Photon.* **4** 15
[47] Xiao S, Wang T, Liu T, Yan X, Li Z and Xu C 2018 *Carbon* **126** 271
[48] Fiori G, Bonaccorso F, Iannaccone G, Palacios T, Neumaier D, Seabaugh A, Banerjee S K and Colombo L 2014 *Nat. Nanotechnol.* **9** 768
[49] Wang Q H, Kalantar-Zadeh K, Kis A, Coleman J N and Strano M S 2012 *Nat. Nanotechnol.* **7** 699
[50] Kuc A, Zibouche N and Heine T 2011 *Phys. Rev. B* **83** 245213
[51] Wang Y, Kim J C, Wu R J, Martinez J, Song X, Yang J, Zhao F, Mkhoyan A, Jeong H Y and Chhowalla M 2019 *Nature* **568** 70
[52] Ma X, Zhang R, An C, Wu S, Hu X and Liu J 2019 *Chin. Phys. B* **28** 037803
[53] Schulman D S, Arnold A J and Das S 2018 *Chem. Soc. Rev.* **47** 3037
[54] Allain A, Kang J, Banerjee K and Kis A 2015 *Nat. Mater.* **14** 1195
[55] Novoselov K S, Geim A K, Morozov S V., Jiang D, Zhang Y, Dubonos S V., Grigorieva I V and Firsov A A 2004 *Science* **306** 666
[56] Schwierz F 2012 *Nat. Nanotechnol.* **5** 487
[57] Geim A K 2009 *Science* **324** 1530
[58] Wang X and Gan X 2017 *Chin. Phys. B* **26** 034203
[59] Neto A H C, Guinea F, Peres N M R, Novoselov K S and Geim A K 2009 *Rev. Mod. Phys.* **81** 109
[60] Wang F, Wang Z, Jiang C, Yin L, Cheng R, Zhan X, Xu K, Wang F, Zhang Y and He J 2017 *Small* **13** 1604298
[61] Koppens F H L, Mueller T, Avouris P, Ferrari A C, Vitiello M S and Polini M 2014 *Nat. Nanotechnol.* **9** 780
[62] Bao Q and Loh K P 2012 *ACS Nano* **6** 3677
[63] Low T and Avouris P 2014 *ACS Nano* **8** 1086
[64] De Abajo F J G 2014 *ACS Photon.* **1** 135
[65] Jablan M, Buljan H and Soljačić M 2009 *Phys. Rev. B* **80** 245435
[66] Koppens F H L, Chang D E and García De Abajo F J 2011 *Nano Lett.* **11** 3370
[67] Wu J Y, Chun Y T, Li S, Zhang T, Wang J, Shrestha P K and Chu D 2018 *Adv. Mater.* **30** 1705880
[68] Wu J Y, Chun Y T, Li S, Zhang T and Chu D 2018 *ACS Appl. Mater. Interfaces* **10** 24613
[69] Lui C H, Frenzel A J, Pilon D V, Lee Y H, Ling X, Akselrod G M, Kong J and Gedik N 2014 *Phys. Rev. Lett.* **113** 166801
[70] Docherty C J, Parkinson P, Joyce H J, Chiu M H, Chen C H, Lee M Y, Li L J, Herz L M and Johnston M B 2014 *ACS Nano* **8** 11147
[71] Kar S, Su Y, Nair R R and Sood A K 2015 *ACS Nano* **9** 12004
[72] Lee S H, Choi M, Kim T T, Lee S, Liu M, Yin X, Choi H K, Lee S S, Choi C G, Choi S Y, Zhang X and Min B 2012 *Nat. Mater.* **11** 936
[73] Miao Z, Wu Q, Li X, He Q, Ding K, An Z, Zhang Y and Zhou L 2015 *Phys. Rev. X* **5** 041027
[74] Zhao Y, Xiao X, Huo Y, Wang Y, Zhang T, Jiang K, Wang J, Fan S and Li Q 2017 *ACS Appl. Mater. Interfaces* **9** 18945
[75] Kim T T, Soon Oh S, Kim H D, Sung Park H, Hess O, Min B and Zhang S 2017 *Sci. Adv.* **3** e1701377
[76] Kindness S J, Almond N W, Wei B, Wallis R, Michailow W, Kamboj V S, Braeuninger-Weimer P, Hofmann S, Beere H E, Ritchie D A and Degl'Innocenti R 2018 *Adv. Opt. Mater.* **6** 1800570
[77] Yadav V S, Ghosh S K, Bhattacharyya S and Das S 2018 *Appl. Opt.* **57** 8720

[78] Zhang M, Wang X X, Cao W Q, Yuan J and Cao M S 2019 *Adv. Opt. Mater.* **7** 1900689

[79] Ryu S, Maultzsch J, Han M Y, Kim P and Brus L E 2011 *ACS Nano* **5** 4123

[80] Liang X, Jung Y S, Wu S, Ismach A, Olynick D L, Cabrini S and Bokor J 2010 *Nano Lett.* **10** 2454

[81] Li J, Sollami Delekta S, Zhang P, Yang S, Lohe M R, Zhuang X, Feng X and Östling M 2017 *ACS Nano* **11** 8249

[82] Minemawari H, Yamada T, Matsui H, Tsutsumi J Y, Haas S, Chiba R, Kumai R and Hasegawa T 2011 *Nature* **475** 364

[83] Yu K, Wang P, Lu G, Chen K H, Bo Z and Chen J 2011 *J. Phys. Chem. Lett.* **2** 537

[84] Kim K S, Zhao Y, Jang H, Lee S Y, Kim J M, Kim K S, Ahn J H, Kim P, Choi J Y and Hong B H 2009 *Nature* **457** 706

[85] Camilli L, Jørgensen J H, Tersoff J, Stoot A C, Balog R, Cassidy A, Sadowski J T, Bøggild P and Hornekær L 2017 *Nat. Commun.* **8** 47

[86] Yatooshi T, Ishikawa A and Tsuruta K 2015 *Appl. Phys. Lett.* **107** 053105

[87] Zhu X, Wang W, Yan W, Larsen M B, Bøggild P, Pedersen T G, Xiao S, Zi J and Mortensen N A 2014 *Nano Lett.* **14** 2907

[88] Thongrattanasiri S, Koppens F H L and García De Abajo F J 2012 *Phys. Rev. Lett.* **108** 047401

[89] Fang Z, Wang Y, Schlather A E, Liu Z, Ajayan P M, García De Abajo F J, Nordlander P, Zhu X and Halas N J 2014 *Nano Lett.* **14** 299

[90] Huidobro P A, Kraft M, Maier S A and Pendry J B 2016 *ACS Nano* **10** 5499

[91] Jessop D S, Kindness S J, Xiao L, Braeuninger-Weimer P, Lin H, Ren Y, Ren C X, Hofmann S, Zeitler J A, Beere H E, Ritchie D A and Degl'Innocenti R 2016 *Appl. Phys. Lett.* **108** 171101

[92] Majumdar A, Kim J, Vuckovic J and Wang F 2013 *Nano Lett.* **13** 515

[93] Shan F, Zhang X Y, Wu J Y and Zhang T 2018 *Chin. Phys. B* **27** 047804

[94] Liu P Q, Luxmoore I J, Mikhailov S A, Savostianova N A, Valmorra F, Faist J and Nash G R 2015 *Nat. Commun.* **6** 8969

[95] Wu J Y, Zhang X Y, Ma X D, Qiu Y P and Zhang T 2015 *RSC Adv.* **5** 95178

[96] Srivastava Y K, Chaturvedi A, Manjappa M, Kumar A, Dayal G, Kloc C and Singh R 2017 *Adv. Opt. Mater.* **5** 1700762

[97] Hu Y, Jiang T, Zhou J, Hao H, Sun H, Ouyang H, Tong M, Tang Y, Li H, You J, Zheng X, Xu Z and Cheng X 2020 *Nano Energy* **68** 104280

[98] Finlayson D M 1990 *Philos. Mag. Lett.* **61** 293

[99] Adler D 1968 *Rev. Mod. Phys.* **40** 714

[100] Morin F J 1959 *Phys. Rev. Lett.* **3** 34

[101] He X, Xu T, Xu X, Zeng Y, Xu J, Sun L, Wang C, Xing H, Wu B, Lu A, Liu D, Chen X and Chu J 2014 *Sci. Rep.* **4** 6544

[102] Guo D, Hu C, Yang Q, Hua H, Li W and Kong C 2014 *Mater. Res. Bull.* **53** 102

[103] He X, Xu J, Xu X, Gu C, Chen F, Wu B, Wang C, Xing H, Chen X and Chu J 2015 *Appl. Phys. Lett.* **106** 093106

[104] Jeong Y G, Bahk Y M and Kim D S 2020 *Adv. Opt. Mater.* **8** 1900548

[105] Wu B H, Xu X F and Wang C R 2016 *Opt. Lett.* **41** 5768

[106] Liu H, Lu J and Wang X R 2018 *Nanotechnology* **29** 24002

[107] Liu M, Hwang H Y, Tao H, Strikwerda A C, Fan K, Keiser G R, Sternbach A J, West K G, Kittiwatanakul S, Lu J, Wolf S A, Omenetto F G, Zhang X, Nelson K A and Averitt R D 2012 *Nature* **487** 345

[108] Thompson Z J, Stickel A, Jeong Y G, Han S, Son B H, Paul M J, Lee B, Mousavian A, Seo G, Kim H T, Lee Y S and Kim D S 2015 *Nano Lett.* **15** 5893

[109] Gray A X, Hoffmann M C, Jeong J, *et al.*, 2018 *Phys. Rev. B* **98** 045104

[110] Liu K, Lee S, Yang S, Delaire O and Wu J 2018 *Mater. Today* **21** 875

[111] Pitchappa P, Kumar A, Prakash S, Jani H, Venkatesan T and Singh R 2019 *Adv. Mater.* **31** 1808157

[112] Li W W, Zhu J J, Xu X F, Jiang K, Hu Z G, Zhu M and Chu J H 2011 *J. Appl. Phys.* **110** 013504

[113] Sang J, Wang P, Meng Y, Xu X, Sun J L, Wang Y, Hua Z, Zheng T, Liu Z, Wang C, Wu B and Chen X 2019 *Jpn. J. Appl. Phys.* **58** 050917

[114] Meng Y, Sang J, Liu Z, Xu X, Tan Z, Wang C, Wu B, Wang C, Cao J and Chen X 2019 *Appl. Surf. Sci.* **470** 168

[115] Wang H, Jian J, Zhang W, Jacob C, Chen A, Wang H and Huang J 2015 *Appl. Phys. Lett.* **107** 102105

[116] Peter A P, Martens K, Rampelberg G, Toeller M, Ablett J M, Meersschaut J, Cuypers D, Franquet A, Detavernier C, Rueff J P, Schaekers M, Van Elshocht S, Jurczak M, Adelmann C and Radu I P 2015 *Adv. Funct. Mater.* **25** 679

[117] Wang D, Zhang L, Gu Y, Mehmood M Q, Gong Y, Srivastava A, Jian L, Venkatesan T, Qiu C W and Hong M 2015 *Sci. Rep.* **5** 15020

[118] Jeong Y G, Han S, Rhie J, Kyoung J S, Choi J W, Park N, Hong S, Kim B J, Kim H T and Kim D S 2015 *Nano Lett.* **15** 6318

[119] Zhou G, Dai P, Wu J, Jin B, Wen Q, Zhu G, Shen Z, Zhang C, Kang L, Xu W, Chen J and Wu P 2017 *Opt. Express* **25** 17322

[120] Wang T, He J, Guo J, Wang X, Feng S, Kuhl F, Becker M, Polity A, Klar P J and Zhang Y 2019 *Opt. Express* **27** 20347

[121] Ding F, Zhong S and Bozhevolnyi S I 2018 *Adv. Opt. Mater.* **6** 1701204

[122] Wen Q Y, Zhang H W, Yang Q H, Xie Y S, Chen K and Liu Y L 2010 *Appl. Phys. Lett.* **97** 021111

[123] Zhao Y, Zhang Y, Shi Q, Liang S, Huang W, Kou W and Yang Z 2018 *ACS Photon.* **5** 3040

[124] Cai H, Chen S, Zou C, Huang Q, Liu Y, Hu X, Fu Z, Zhao Y, He H and Lu Y 2018 *Adv. Opt. Mater.* **6** 1800257

[125] Zhang Y, Qiao S, Sun L, Shi Q W, Huang W, Li L and Yang Z 2014 *Opt. Express* **22** 11070

[126] Liu L, Kang L, Mayer T S and Werner D H 2016 *Nat. Commun.* **7** 13236

[127] Rensberg J, Zhang S, Zhou Y, McLeod A S, Schwarz C, Goldflam M, Liu M, Kerbusch J, Nawrodt R, Ramanathan S, Basov D N, Capasso F, Ronning C and Kats M A 2016 *Nano Lett.* **16** 1050

[128] Muskens O L, Bergamini L, Wang Y, Gaskell J M, Zabala N, De Groot C H, Sheel D W and Aizpurua J 2016 *Light: Sci. Appl.* **5** e16173

[129] Lei D Y, Appavoo K, Ligmajer F, Sonnefraud Y, Haglund R F and Maier S A 2015 *ACS Photon.* **2** 1306

[130] Wang B X and Wang G Z 2016 *IEEE Photon. J.* **8** 5502408

[131] Anlage S M 2011 *J. Opt.* **13** 024001

[132] Jin B, Zhang C, Engelbrecht S, Pimenov A, Wu J, Xu Q, Cao C, Chen J, Xu W, Kang L, Wu P 2010 *Opt. Express* **18** 17504

[133] Zhang C, Jin B, Han J, Kawayama I, Murakami H, Wu J, Kang L, Chen J, Wu P and Tonouchi M 2013 *Appl. Phys. Lett.* **102** 081121

[134] Li C, Zhang C, Hu G, Zhou G, Jiang S, Jiang C, Zhu G, Jin B, Kang L, Xu W, Chen J and Wu P 2016 *Appl. Phys. Lett.* **109** 022601

[135] Gu J, Singh R, Tian Z, Cao W, Xing Q, He M, Zhang J W, Han J, Chen H T and Zhang W 2010 *Appl. Phys. Lett.* **97** 071102

[136] Jung P, Ustinov A V. and Anlage S M 2014 *Supercond. Sci. Technol.* **27** 073001

[137] Srivastava Y K and Singh R 2017 *J. Appl. Phys.* **122** 183104

[138] Zhang C H, Wu J B, Jin B B, Ji Z M, Kang L, Xu W W, Chen J, Tonouchi M and Wu P 2012 *Opt. Express* **20** 42

[139] Liu X, Guo W, Wang Y, Dai M, Wei L F, Dober B, McKenney C M, Hilton G C, Hubmayr J, Austermann J E, Ullom J N, Gao J and Vissers M R 2017 *Appl. Phys. Lett.* **111** 252601

[140] Guo W, Liu X, Wang Y, Wei Q, Wei L F, Hubmayr J, Fowler J, Ullom J, Vale L, Vissers M R and Gao J 2017 *Appl. Phys. Lett.* **110** 212601

[141] Wu J, Jin B, Xue Y, Zhang C, Dai H, Zhang L, Cao C, Kang L, Xu W, Chen J and Wu P 2011 *Opt. Express* **19** 12021

[142] Chen H T, Yang H, Singh R, O'Hara J F, Azad A K, Trugman S A, Jia Q X and Taylor A J 2010 *Phys. Rev. Lett.* **105** 247402

[143] Wu J, Jin B, Wan J, Liang L, Zhang Y, Jia T, Cao C, Kang L, Xu W, Chen J and Wu P 2011 *Appl. Phys. Lett.* **99** 161113

[144] Srivastava Y K, Manjappa M, Cong L, Krishnamoorthy H N S, Savinov V, Pitchappa P and Singh R 2018 *Adv. Mater.* **30** 1801257

[145] Li C, Wu J, Jiang S, Su R, Zhang C, Jiang C, Zhou G, Jin B, Kang L, Xu W, Chen J and Wu P 2017 *Appl. Phys. Lett.* **111** 092601

[146] Grady N K, Perkins B G, Hwang H Y, Brandt N C, Torchinsky D, Singh R, Yan L, Trugman D, Trugman S A, Jia Q X, Taylor A J, Nelson K A and Chen H T 2013 *New J. Phys.* **15** 105016

[147] Müller M M, Maier B, Rockstuhl C and Hochbruck M 2019 *Phys. Rev. B* **99** 075401

[148] Srivastava Y K 2018 *Superconductor Terahertz metamaterials* (Ph.D dissertation) (Sigapore: Nanyang Technological University)

[149] Stav T, Faerman A, Maguid E, Oren D, Kleiner V, Hasman E and Segev M 2018 *Science* **361** 1101

[150] Ming Y, Zhang W, Tang J, Liu Y, Xia Z, Liu Y and Lu Y Q 2020 *Laser Photonics Rev.* **14** 1900146

[151] Fan F, Chen S and Chang S J 2017 *IEEE J. Sel. Top. Quantum Electron.* **23** 8500111

[152] Belotelov V I, Kreilkamp L E, Akimov I A, Kalish A N, Bykov D A, Kasture S, Yallapragada V J, Gopal A V, Grishin A M, Khartsev S I, Nur-E-Alam M, Vasiliev M, Doskolovich L L, Yakovlev D R, Alameh K, Zvezdin A K and Bayer M 2013 *Nat. Commun.* **4** 2128
[153] Zubritskaya I, Maccaferri N, Inchausti Ezeiza X, Vavassori P and Dmitriev A 2018 *Nano Lett.* **18** 302
[154] Shimano R, Yumoto G, Yoo J Y, Matsunaga R, Tanabe S, Hibino H, Morimoto T and Aoki H 2013 *Nat. Commun.* **4** 1841
[155] Chen S, Fan F, Wang X, Wu P, Zhang H and Chang S 2015 *Opt. Express* **23** 1015
[156] Chen S, Fan F, He X, Chen M and Chang S 2015 *Appl. Opt.* **54** 9177
[157] Ottomaniello A, Zanotto S, Baldacci L, Pitanti A, Bianco F and Tredicucci A 2018 *Opt. Express* **26** 3328
[158] Watts C M, Shrekenhamer D, Montoya J, Lipworth G, Hunt J, Sleasman T, Krishna S, Smith D R and Padilla W J 2014 *Nat. Photon.* **8** 605
[159] Bao L and Cui T J 2020 *Microw. Opt. Technol. Lett.* **62** 9
[160] Sun D, Lai J W, Ma J C, Wang Q S and Liu J 2017 *Chin. Phys. B* **26** 037801
[161] Shcherbakov M R, Eilenberger F and Staude I 2019 *J. Appl. Phys.* **126** 085705
[162] Jiang N, Zhuo X and Wang J 2018 *Chem. Rev.* **118** 3054
[163] Bekenstein R, Pikovski I, Pichler H, Shahmoon E, Yelin S F and Lukin M D 2020 *Nat. Phys.* **16** 676